



ISSN: 2230-9926

Available online at <http://www.journalijdr.com>

IJDR

International Journal of Development Research

Vol. 12, Issue, 05, pp. 55781-55787, May, 2022

<https://doi.org/10.37118/ijdr.24475.05.2022>



RESEARCH ARTICLE

OPEN ACCESS

RESEARCH ON THE PHYSICAL MECHANISM OF THE MAGNETIZATION REVERSAL PHENOMENON OF FERROMAGNETIC SPECIMENS

Daluan Wang and *Shangkun Ren

Key Laboratory of Non-destructive Testing Technology of Ministry of Education, School of Testing and Optoelectronic Engineering, Nanchang Hangkong University, Nanchang 330063, Jiangxi, China

ARTICLE INFO

Article History:

Received 19th February, 2022

Received in revised form

26th March, 2022

Accepted 21st April, 2022

Published online 20th May, 2022

Key Words:

Metal Magnetic Memory Detection; ANSYS Finite Element Simulation; force-magnetic Coupling; Magnetization Reversal model; Stress-Effective Field Model; Stress-Permeability Model.

ABSTRACT

In order to study the physical mechanism of the magnetization reversal phenomenon of ferromagnetic specimens, the Q235 steel plate was simulated by ANSYS simulation software. When the maximum stress is greater than 252MPa, the magnetization reversal phenomenon occurs. Starting from the principle of minimum energy, combined with the external magnetic field energy and stress energy, a magnetization reversal model based on the principle of minimum energy is established, which explains the phenomenon of magnetization inversion from a microscopic perspective; at the same time, a stress-effective field model and a stress-permeability model reflects the change of the macroscopic magnetization through the change of the microscopic effective field and magnetic permeability. The research shows that the three mathematical models can reflect the magnetization reversal phenomenon of stress, which lays a theoretical foundation for the in-depth research on the quantitative detection of metal magnetic memory.

*Corresponding author: *Shangkun Ren*,

Copyright © 2022, Daluan Wang and Shangkun Ren. This is an open access article distributed under the Creative Commons Attribution License, which permits unrestricted use, distribution, and reproduction in any medium, provided the original work is properly cited.

Citation: Daluan Wang and Shangkun Ren. "Research on the Physical Mechanism of the Magnetization Reversal Phenomenon of Ferromagnetic Specimens", *International Journal of Development Research*, 12, (05), 55781-55787.

INTRODUCTION

In 1994, Russian professor DOUBOV first proposed the metal magnetic memory detection technology [Ren Jilin, 2016]. The metal magnetic memory detection technology uses the geomagnetic field as the excitation. Under the combined action of the stress and the geomagnetic field, the magnetostrictive strain is generated inside the ferromagnetic specimen, and the spontaneous magnetization direction of the magnetic domain inside the ferromagnetic material is changed, resulting in stress concentration at the defect. , these phenomena are macroscopically manifested as the generation of leakage magnetic fields. Due to the advantages of metal magnetic memory detection technology without excitation source, green environmental protection, no pollution, and high detection sensitivity, since the advent of this technology, it has attracted the attention of a large number of scholars at home and abroad: Jiles [Jiles, 1995] et al proposed the law of proximity, and established Models of magnetization, external magnetic field, and stress are presented. Ren Shangkun [Ren Shangkun, 2019] et al. carried out a series of fatigue tests for weld defects, combined with radiographic detection technology, and established a fatigue damage model with magnetic field vector gradient characteristics as damage parameters. Yang Lijian [2021] and others proposed a pipeline stress detection method based on the force-magnetic coupling effect and the molecular current theory. Chen Shangong [2021] and others conducted fatigue tests on the specimens, analyzed the metal magnetic memory signals of the specimen surfaces under different fatigue loads, and established a fatigue damage model. With the development of metal magnetic memory technology, scholars at home and abroad have done a lot of research and experiments on the force-magnetic coupling, but there are relatively few studies on the magnetization reversal effect (Li, 2013; Ren Shangkun, 2010; Ren Shangkun, 2008; Ren Shangkun, 2004). In this paper, the magnetization reversal effect is further studied from the two aspects of finite element simulation and theoretical analysis: using the ANSYS finite element simulation software, the change law of the magnetic memory signal of the ferromagnetic specimen under tensile stress is simulated. The phenomenon of magnetization reversal and the change of the extremum point of magnetization reversal of ferromagnetic specimens with the change of the maximum tensile stress are two phenomena.

Microscopic models are established to explain the above two phenomena, and the magnetization reversal is given. The physical mechanism of the effect. The essence of the magnetization reversal effect is that the change of the applied stress causes the change of the internal magnetization of the material, that is, the magnetic effect of the stress. In the actual detection process, since the magnetization of the material is difficult to directly measure, this paper measures the leakage magnetic field strength of the test piece to reflect the change characteristics of the magnetization inside the material [Al-Naemi, 2006].

ANSYS finite element simulation

ANSYS Simulation Process: The simulation uses Q235 steel plate as the research object, the thickness of the test piece is 3mm, its size is shown in Fig.1, and the technical parameters are shown in Table 1. A detection path with a length of 180mm was taken in the middle of the specimen, and the value of the magnetic memory normal component $H(y)$ under different stresses at point M on the path was extracted by APDL language. The mesh adopts tetrahedral mesh, and the division method adopts free division. In order to ensure the calculation accuracy while taking into account the calculation speed, the mesh is refined by artificial mesh division near the M point. The mesh division is shown in Fig.2.

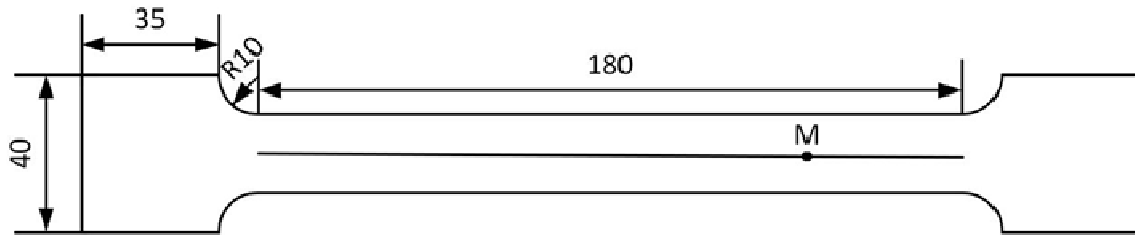


Fig. 1. Q235 dimension drawing (unit is mm)

Table 1. Q235 steel plate technical parameters

参数	$E(\text{GPa})$	ν	$\sigma_s(\text{MPa})$	$\sigma_m(\text{MPa})$	μ_T
参考值	203	0.28	280	420	285

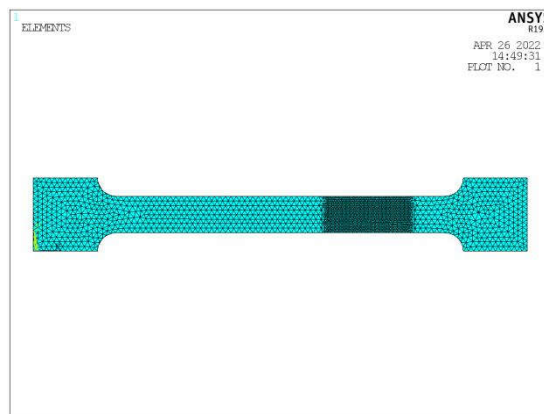


Fig. 2. Q235 steel plate finite element partition model

The simulation adopts the sequential coupling method, including nonlinear static analysis and magnetostatic analysis. Firstly, the nonlinear static analysis is performed, the element type is solid185, the left end of the specimen is restrained, and the right end is subjected to tensile load, which is applied in four stages: the first stage is the elastic stage, and the tensile load is applied from 0 to 162MPa; The second stage is the plastic stage, and the tensile load is applied from 0 to 252MPa; the third stage is the plastic stage, and the tensile load is applied from 0 to 306MPa; the fourth stage is near the tensile strength, and the tensile load is applied from 0 to 378MPa. stage restarts the simulation, the four stages are not related. After the statics simulation is over, the element stress is extracted into the array and converted into the element permeability in preparation for the magnetostatic analysis. The magnetostatic analysis adopts solid95 element, and the nodal degree of freedom is MAG. An air domain is established in the outer layer of the specimen to simulate the terrestrial magnetic field. The magnetic potential on the left side of the air domain is 0, and the magnetic potential on the right side is 39.8A/m. Use the *VREAD and EMODIF commands to assign the unit permeability to each unit, and use APDL language to extract the $H(y)$ value of the M point under the action of the geomagnetic field. The lift-off height is set to 0, and the relevant results are saved.

ANSYS Simulation Results: Fig.3 shows the relationship between the magnetic memory signal value $H(y)$ at point M and the stress when the maximum stress of the Q235 steel plate is 162MPa. In fact, when the ferromagnetic specimen is subjected to tensile stress, the specimen is approximately magnetized into a magnet, and the value of the magnetic memory signal at both ends of the specimen shows an opposite variation law, and the farther from the midpoint of the specimen, the magnetic memory signal bigger. The M point is located between the midpoint of the specimen and the right end point, which can not only generate a relatively obvious magnetic memory signal value, but also reduce the end interference. It can be seen from Fig.3 that in the elastic stage, the value of the magnetic memory signal at point M increases with the increase of the stress, which is approximately linear with the stress, and there is no magnetization reversal phenomenon. When the tensile load is close to the yield strength of the specimen, as shown in Fig. 4: the value of the magnetic memory signal first increases with the increase of the tensile load. When the tensile load reaches 84MPa, the value of the magnetic memory signal increases with the increase of the tensile load. The magnetization reversal phenomenon appears obvious. When the tensile load further increases, the specimen enters the plastic stage, as shown in Fig.5: the value of the magnetic memory signal increases with the increase of the tensile load.

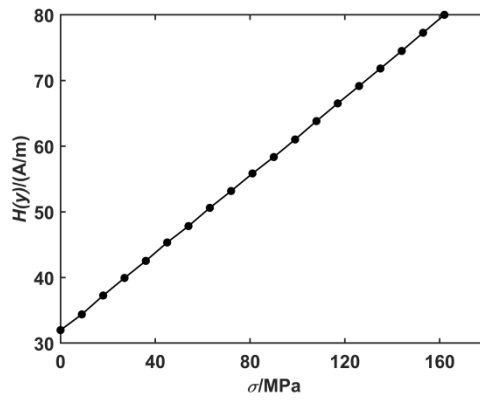


Fig. 3. The relationship between $H(y)$ and stress when the maximum tensile stress is 162MPa

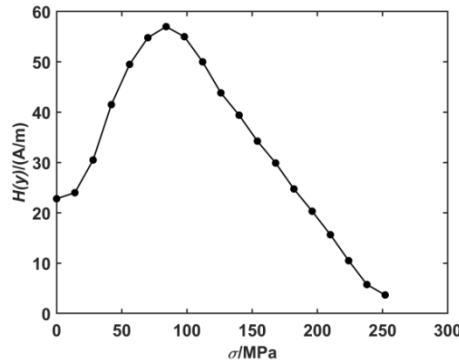


Fig. 4. The relationship between $H(y)$ and stress when the maximum tensile stress is 252MPa

When the tensile load reaches 170MPa, the value of the magnetic memory signal increases with the tensile load. The magnetization reversal phenomenon appears, and with the increase of the maximum tensile stress, the extreme point of the magnetization reversal keeps moving to the right.

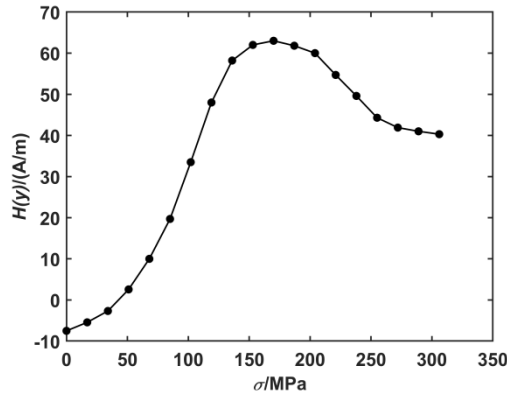


Fig. 5. The relationship between $H(y)$ and stress when the maximum tensile stress is 306MPa

It can be seen from Fig.6 that when the maximum tensile load is close to the tensile strength of the specimen, the magnetization reversal phenomenon occurs when the tensile load is 273MPa, and the extreme point of the magnetization reversal moves further to the right, which is the same as that in Fig. 4 and Fig. 5. have similar rules.

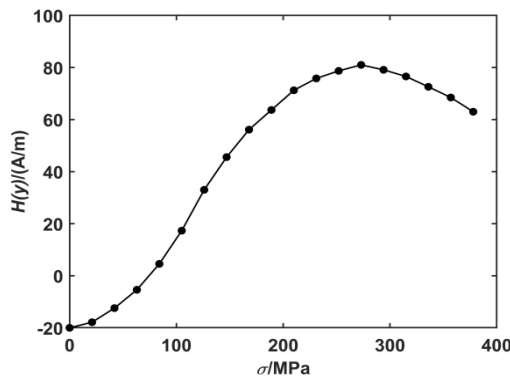


Fig. 6. The relationship between $H(y)$ and stress when the maximum tensile stress is 378MPa

Theoretical Model Research and Analysis of Magnetization Inversion Effect

A magnetization reversal model based on the principle of least energy: Under the combined action of the tensile stress coaxial with the external magnetic field and the external magnetic field, the Gibbs free energy of the ferromagnetic material is mainly composed of the external magnetic field energy E_H and stress energy E_σ [Zhang Peng, 2013]:

$$E = E_H + E_\sigma = -\mu_0 MH \cos \theta - \frac{3}{2} \lambda_s \sigma \cos^2 \theta \quad (1)$$

In the formula: E is the Gibbs free energy of the material; E_H is the external magnetic field energy; E_σ is the stress energy; M is the magnetization; H is the external magnetic field; μ_0 is the vacuum permeability; θ is the angle between the magnetization direction of the internal magnetic domain of the material and the external magnetic field; λ_s is the saturation magnetostriction coefficient; σ is the stress. According to the principle of minimum energy, when a ferromagnetic material is subjected to the combined action of stress and external magnetic field, the change trend of the magnetization direction of the internal magnetic domain of the material and the angle between the external magnetic field always minimizes the free energy of the material, so there are:

$$\frac{dE}{d\theta} = \mu_0 MH \sin \theta + 3 \lambda_s \sigma \cos \theta \sin \theta = 0 \quad (2)$$

When the stress is tensile stress, σ is greater than 0. It can be obtained from formula (2) that when $\theta = \arccos\left(-\frac{\mu_0 MH}{3\lambda_s \sigma}\right)$ or $\theta = \pi - \arccos\left(-\frac{\mu_0 MH}{3\lambda_s \sigma}\right)$, The Gibbs free energy E has an extreme point, which is the minimum point of E and the maximum point of E . Assuming that the applied stress and the external magnetic field are constants, then the relationship between the free energy E and θ is shown in Fig.7.

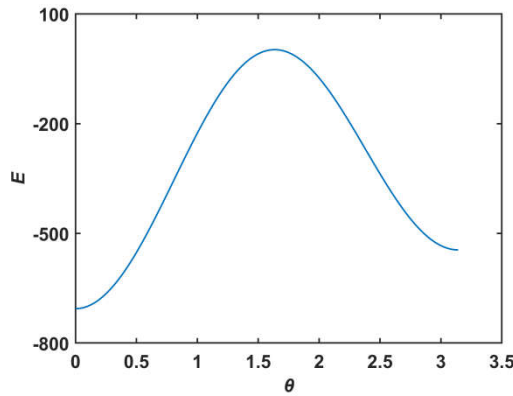


Fig. 7. The relationship between E and θ

When a ferromagnetic material is subjected to external stress, a magnetostrictive effect occurs inside it. When the tensile stress is small, the material is in the elastic stage. After the tensile stress is removed, the interior of the material returns to the initial state, so there is no magnetization reversal phenomenon in the elastic stage. When the tensile stress increases, reaching or even exceeding the yield strength of the material, the spontaneous magnetization direction of the magnetic domain walls inside the material changes irreversibly. As shown in Fig. 7, as the stress increases, the spontaneous magnetization direction of the magnetic domain wall gradually approaches the stress direction. During this process, the spontaneous magnetization direction of the magnetic domain with the angle greater than $\arccos\left(-\frac{\mu_0 MH}{3\lambda_s \sigma}\right)$ gradually approaches the stress direction. The Gibbs free energy first increases and then decreases, and the macroscopic performance is that the magnetization reversal phenomenon occurs in the ferromagnetic specimen.

Stress Equivalent Magnetic Field Model for Stress Magnetization Reversal: When a ferromagnetic material is subjected to tensile stress, the effect of the stress can be equivalent to the stress field H_σ [JILES, 2004]:

$$H_\sigma = \frac{3\sigma}{2\mu_0} \left(\frac{d\lambda}{dM} \right) (\cos^2 \theta - \nu \sin^2 \theta) \quad (3)$$

In the formula: H_σ is the stress field; λ is the magnetostrictive coefficient; μ_0 is the magnetic permeability in vacuum; ν is the Poisson's ratio; θ is the angle between the stress and the external magnetic field. The magnetostriction coefficient λ is related to the stress σ and the magnetization M , and is an even function of M [13]. The Taylor series is used to expand the λ , and the higher-order terms are omitted to simplify the calculation, as follows:

$$\lambda(\sigma, M) = (m + n\sigma)M^2 \quad (4)$$

The equivalent field of the ferromagnetic specimen under the combined action of stress and external magnetic field is:

$$H_e = H + \alpha M + \frac{3\sigma}{2\mu_0} \left(\frac{d\lambda}{dM} \right) (\cos^2 \theta - v \sin^2 \theta) \quad (5)$$

In the formula: H_e is the effective field; α is the Weiss molecular field coefficient, which represents the interaction between the magnetic domains. Under the premise of linear response, the magnetization of the ferromagnetic specimen can be expressed as:

$$M = \chi H_e \quad (6)$$

In the formula: χ represents the magnetic susceptibility of the ferromagnetic material. Substituting equations (4) and (6) into equation (5), the relationship between effective field H_e and stress σ is obtained:

$$H_e = H + \frac{\alpha \chi H + \frac{3\sigma}{\mu_0} (m + n\sigma) \chi H (\cos^2 \theta - v \sin^2 \theta)}{1 - \chi \left[\alpha + \frac{3}{\mu_0} (m\sigma + n\sigma^2) (\cos^2 \theta - v \sin^2 \theta) \right]} \quad (7)$$

The model parameters are as follows: $H = 40 \text{ A/m}$, $\alpha = 0.001$, $\chi = 500$, $\mu_0 = 4\pi \times 10^{-7} \text{ N/A}^2$, $v = 0.28$, $\theta = 27^\circ$. (7) can be

simplified as:

$$H_e = 40 + \frac{20 + 3.53 \times 10^{10} (m\sigma + n\sigma^2)}{0.5 - 8.76 \times 10^8 (m\sigma + n\sigma^2)} \quad (8)$$

Formula (8) takes the derivative of the stress σ and sets its derivative to 0, the extreme point of the effective field H_e can be obtained as $\sigma_a = -m/2n$, and σ_a corresponds to the magnetization reversal point in Fig.4, as follows: $n = -6 \times 10^{-9} \text{ m}$. According to [14], the value of m is $7 \times 10^{-18} \text{ m}^2/\text{A}^2$, at this time $n = -4.2 \times 10^{-26}$, Taking $n_1 = -3 \times 10^{-26}$, $n_2 = -4 \times 10^{-26}$, $n_3 = -5 \times 10^{-26}$, the relationship between the effective field H_e and the stress σ is shown in Fig.8: With the increase of stress, the effective field shows a trend of first increasing and then decreasing, and there is an extreme point. As n increases, the extreme point moves to the right, and the position of the extreme point is affected by m/n , which is related to the maximum stress on the ferromagnetic specimen. As the maximum stress increases, the magnetization reversal point shifts to high stress locations. When m/n remains unchanged, the larger the n value, the more obvious the force-magnetic coupling effect of the material. It can be seen that the magnetization reversal phenomenon of the ferromagnetic specimen is related to the magnetostrictive parameters m and n , and the stress-effective field model can well explain the magnetization reversal phenomenon.

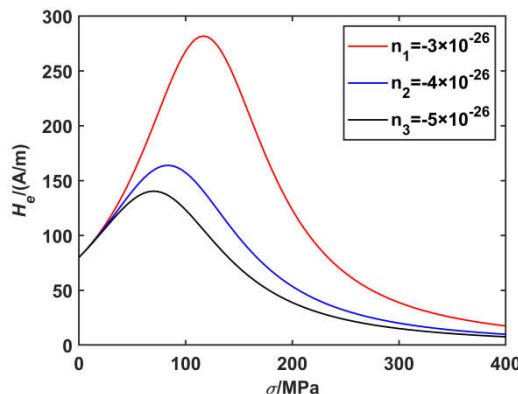


Fig. 8. The relationship between effective field H_e and stress σ

Magnetic permeability model for stress magnetization reversal: Under the combined action of stress and external magnetic field, the ferromagnetic specimen will have a piezomagnetic effect inside, which will lead to corresponding changes in the magnetic domain structure. The final performance is that the magnetic permeability will change with the change of stress. The relationship between the strength B , the magnetic field strength H , and the magnetization strength M is:

$$B = \mu_0 (H + M) \quad (9)$$

From equations (5) and (6), we can get:

$$M = \frac{\chi H}{1 - \chi \left[\alpha + \frac{3}{\mu_0} (m\sigma + n\sigma^2) (\cos^2 \theta - v \sin^2 \theta) \right]} \tag{10}$$

Substituting Equation (9) into Equation (10), the relationship between the magnetic induction intensity B and the external magnetic field H and stress is obtained:

$$B = \frac{\mu_0 \chi H}{1 - \chi \left[\alpha + \frac{3}{\mu_0} (m\sigma + n\sigma^2) (\cos \theta - v \sin^2 \theta) \right]} + \mu_0 H \tag{11}$$

Formula (11) is derived from the external magnetic field H to obtain the permeability under the influence of stress only:

$$\mu_\sigma = \frac{\mu_0 \chi}{1 - \chi \left[\alpha + \frac{3}{\mu_0} (m\sigma + n\sigma^2) (\cos \theta - v \sin^2 \theta) \right]} + \mu_0 \tag{12}$$

Set some parameters as follows: $\theta = 0, \mu_0 = 1$, (12) can be simplified as:

$$\mu_\sigma = 1 + \frac{1}{\frac{1}{\chi} - \alpha - 3(m\sigma + n\sigma^2)} = 1 + \frac{b}{(a\sigma + 1)[k(\sigma - 1) + 1]} \tag{13}$$

According to the equivalent infinitesimal formula: when $\sigma \rightarrow 0, 1 + a\sigma \sim e^{a\sigma}, (1 + \sigma)^n - 1 \sim n\sigma$, Then (13) can be simplified as:

$$\mu_\sigma = 1 + b\sigma^{-k} e^{-a\sigma} \tag{14}$$

Equation (13) takes the derivative of stress σ and sets its derivative to 0, the extreme point of permeability μ_σ can be obtained as $\sigma_e = -k/a$, and σ_e corresponds to the magnetization reversal point in Fig.4, as follows: $k = -84a$. k, b can be calculated from Reference [15] directly gives: $k = 2.64332, b = 2 \times 10^{-5}$, and $a = -0.03148$ can be obtained from k . Taking $a_1 = -0.02148, a_2 = -0.03148$ and $a_3 = -0.04148$, the relationship between permeability μ and stress σ is shown in Fig.9; taking $b_1 = 2 \times 10^{-5}, b_2 = 2.3 \times 10^{-5}, b_3 = 2.6 \times 10^{-5}$ and $b_4 = 2.9 \times 10^{-5}$, the relationship between permeability μ and stress σ is shown in Fig.10.

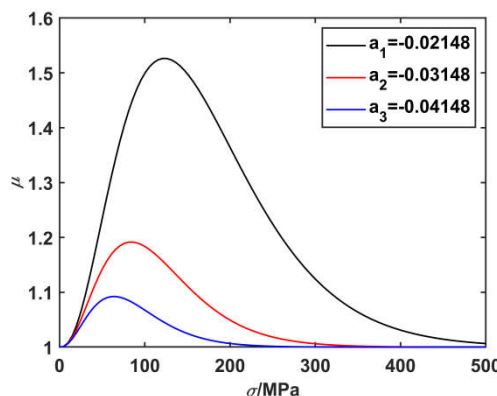


Fig. 9 The effect of fitting coefficient a on permeability

It can be seen from Fig.9 that with the increase of the stress σ , the stress-permeability curve shows a trend of first increasing and then decreasing, and an extreme point appears; the fitting coefficient a increases with the increase of the maximum stress on the material. With the increase of a , the magnetic effect of stress is obviously enhanced, and the extreme point is obviously shifted to the right, corresponding to the magnetization reversal point of the material. It can be seen from Fig.10 that when k/a remains unchanged, as b increases, the stress-permeability curve rises slowly, and the extreme point of the curve remains unchanged. It can be seen that the fitting coefficient b is related to the properties of the material itself and has nothing to do with the applied stress; while the fitting coefficient a is affected by the maximum stress, and the force-magnetic coupling effect on the material is stronger than that of the fitting coefficient b . The permeability of the material can be equivalent to the magnetization of the external magnetic field, so the stress-permeability model can reflect the magnetization reversal phenomenon of the material.

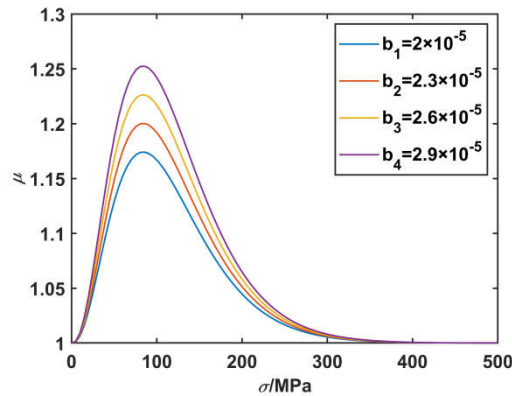


Fig. 10. The effect of fitting coefficient b on permeability

CONCLUSION

Through the simulation test of Q235 steel plate, it is found that there is obvious magnetization reversal phenomenon. By measuring the value of the leakage magnetic field component at the fixed point under different stresses, it is found that when the maximum stress is 162MPa, the relationship between the magnetic field value and the stress is approximately a straight line, and there is no magnetization reversal phenomenon; when the maximum stress is greater than 252MPa, the magnetic field value and the relationship of stress becomes a broken line, which shows a trend of increasing first and then decreasing. There is an obvious magnetization reversal phenomenon, and with the increase of the maximum stress, the magnetization reversal point keeps moving to the right. Starting from the principle of minimum energy, combined with the external magnetic field energy and stress energy, the models of free energy E and θ are established, and the magnetization reversal effect is explained microscopically. At the same time, the stress-effective field model and the stress-permeability model are established, and the influencing factors of the magnetization reversal are given. The two models can well reflect the magnetization reversal effect of the material.

REFERENCES

- Ren Jilin, Liu Haichao, Song Kai. The Rise and Development of Metal Magnetic Memory Testing Technology[J]. Nondestructive Testing, 2016, 38(11): 7-15.
- JILES D C. Theory of the magnetomechanical effect [J]. Journal of Physics D Applied Physics, 1995, 28 (8) : 1537-1546.
- Ren Shangkun, Zu ruili. Fatigue test of welds with defects based on magnetic memory technology[J]. Acta Aeronautica ET Astronautica Sinica, 2019, 40(03): 251-262.
- Yang Lijian, Zheng Fuyin, Gao Songwei, et al. An analytical model of electromagnetic stress-s detection for pipeline based on magneto-mechanical coupling model[J]. Chinese Journal of Scientific Instrument, 2021, 41(08): 249-258
- Cheng Shangong, Zong Xuemei, Huang Haihong, et al. Fatigue damage evaluation of used parts based on metal magnetic memory testing[J]. Nondestructive Testing, 2021, 43(1): 29-33
- Li yi, Ren Shangkun. Magnetization Reversal of Ferromagnetic Specimens Under the Static Tension Conditions[J]. Journal of Iron and Steel Research, 2013, 25(03): 30-33.
- Ren Shangkun, Zhou LI, Fu Renzhen. Magnetizing Reversion Effect of Ferromagnetic Specimens in Process of Stress-Magnetizing[J]. Journal of Iron and Steel Research, 2010, 22(12): 48-52
- Ren Shangkun, Ren Jilin, Wu Guanhua, et al. Studies on the Relationship Between Stress in Different Range with Magnetic Effects for 45 Steel Components[J]. Nondestructive Testing, 2008(04): 244-247+254
- Ren Shangkun, Lin Tianhua, Yang Yaling, et al. STRESS-MAGNETIC EFFECTS FOR 45 COLD ROLL STEEL[J]. Physical Testing and Chemical Analysis Part A: Physical Testing, 2008, 44(12): 677-679+683
- Al-Naemi FI, Hall JP, Moses AJ. FEM modelling techniques of magnetic flux leakage-type NDT for ferromagnetic plate inspections. [J]. Journal of Magnetism and Magnetic Materials, 2006, 304(2): e790-e793.
- Zhang Peng, Liu Lin, Chen Weimin. Analysis of characteristics and key influencing factors in magnetomechanical behavior for cable stress monitoring[J]. Acta Physica Sinica, 2013, 62(17): 454-462.
- JILES D C, LI L. A new approach to modeling the magnetomechanical effect[J]. Journal of Applied Physics, 2004, 95(11): 7085-7060
- JILES D C, ATHERTON D L. Theory of the Magnetisation Process in Ferromagnets and Its Application to the Magnetomechanical Effect[J]. Journal of Physics D : Applied Physics, 1984, 17(6): 1265.
- Liu Qingyou, Luo Xu, Zhu Haiyan, et al. Modeling plastic deformation effect on the hysteresis loops of ferromagnetic materials based on modified Jiles-Atherton model[J]. Acta Physica Sinica, 2017, 66(10): 297-306.
- Huang Yin. Research on force-magnetic effect of Ferromagnetic specimen Based on Metal magnetic memory[D]. NanChang Hangkong University, 2016.
